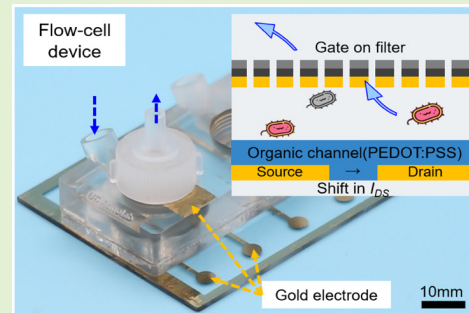


Flow-Cell Sensor for Bacteria Detection Using Gate-Modified Organic Electrochemical Transistor

Jingchu Huang¹, Member, IEEE, Daewoo Han¹, and Andrew J. Steckl¹, Life Fellow, IEEE

Abstract—Organic electrochemical transistors (OECTs) have been previously demonstrated in the sensing of cells and metabolic products. In this study, we report a novel approach on the universal detection of bacterial contamination in home liquid goods through the utilization of a microfluidic flow cell that has been integrated with OECT technology. The flow-cell device has been developed for the purpose of detecting minimal concentration ($\sim 10^3$ CFU/mL) of several bacterium types [*Escherichia coli* (*E. Coli*), *Pseudomonas fluorescens* (*P. flu*), and *Staphylococcus aureus* (*S. au*)] in various commercial household liquid product blends (see Air Febreze, Tide, and Old SPICE Bodywash). This process can be completed in a testing period of 1 h or less and does not require amplification or a designated binding agent. The flow-cell configuration uses a microporous filter membrane (Au-coated polyethylene terephthalate (PETE), 0.2- μm pore diameter) designed to concentrate the bacteria within the chamber. The membrane also functions as a gate electrode for the operation of OECT. The presence of bacteria on the gate filter membrane leads to an increase in the total effective gate voltage (V_{eff}), which in turn causes a decrease in the OECT source–drain channel current (I_{DS}). Based on the shift of I_{DS} , the OECT provides good discrimination between bacteria and sterile solutions (0.4-mA difference). The OECT transconductance (g_m) exhibits a maximum value at different levels of V_{GS} for sterile and bacteria solutions. This approach exhibits potential for biosensing systems that will enable real-time monitoring at the production line.

Index Terms—Bacteria, flow cell, liquid products, organic electrochemical transistor (OECT), sensor.



I. INTRODUCTION

HOME liquid products, such as clothes cleansers, body cleansers, and air fresheners, are widely used in numerous aspects of daily life with the expectation that they are bacteria-free. The liquid state of these products makes it easier for microorganisms to proliferate and, in the event of contamination with pathogenic bacteria, can lead to the manifestation of diverse illnesses [1]. Microbiologists use a technique known as the “standard plate count” [2] to detect bacteria and estimate the population density in a bouillon by plating a small, diluted sample and counting the number of bacterial colonies after 48 h of incubation. In recent years, the polymerase chain reaction (PCR) method [3] and the enzyme-linked immunosor-

bent assay (ELISA) [4] have been utilized for biosensing microorganisms with high sensitivity and specificity. Although these techniques are very sensitive and accurate, they tend to be time consuming, requiring expert processing, and relatively expensive. In addition, transfer of cells/bacteria and sample enrichment necessitate biosafety environments, limiting the potential for test-on-set and real-time monitoring [2]. Detecting potential bacteria contamination issues in household liquid products in “real time” (whether during the manufacturing process or consumer use) requires a detection method that fulfills several requirements: broad bacteria detection, simplicity, affordability, sensitivity, and portability.

The organic electrochemical transistor (OECT) is an attractive device for sensing biological species due to its high sensitivity to ion concentration changes in the liquid state [5], [6], [7]. OECT is a thin-film transistor with an organic semiconductor channel between source and drain electrodes. OECTs have been reported to be effective in various cases of biosensing signals, including the presence of ions (such as potassium [8] and calcium [9]), glucose [10], and DNA [11]. Two methods are generally available for using OECT-based detection: channel sensing [12], [13], [14] and gate electrode

Manuscript received 6 October 2023; revised 27 November 2023, 29 November 2023, and 28 December 2023; accepted 4 January 2024. Date of publication 12 January 2024; date of current version 29 February 2024. This work was supported by Procter & Gamble Company. The associate editor coordinating the review of this article and approving it for publication was Dr. Levent Yobas. (Corresponding author: Andrew J. Steckl.)

The authors are with the Department of Electrical and Computer Engineering, University of Cincinnati, Cincinnati, OH 45221 USA (e-mail: a.steckl@uc.edu).

Digital Object Identifier 10.1109/JSEN.2024.3350969

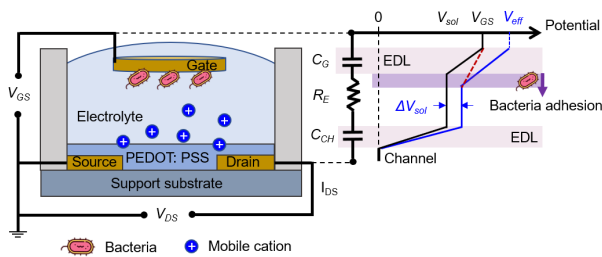


Fig. 1. OECT microorganism detection mechanics: OECT schematic and corresponding ionic circuit; potential drop from gate electrode across EDLs and electrolyte to OECT channel. Adhesion of bacteria on the gate electrode results in a solution (electrolyte) voltage change ΔV_{sol} , and this change can be also represented through the change of effective gate voltage V_{eff} , which is the gate voltage required to produce the same electrolyte potential without bacteria-gate attachment.

sensing [15]. In channel sensing, bacteria directly affect the OECT channel current by physical contact. This sensing method for bacteria is used in the majority of published works, due to its direct response to ion migration in electrolytes [16] and well-understood working mechanism [5], [17]. A limitation of the channel sensing approach is the fact that surface chemistry and modification of the channel can disrupt the adhesion and electronic properties of the organic layer [18]. In the second method, the gate electrode serves as an alternative sensing location. Gate sensing has several attractive features, including flexibility to vary the electrode material [19], incorporation of binding biochemical agents [20], and making chemical modifications [14], [21] without affecting the organic semiconductor layer. Recent research on OECT gate biosensing has been reported for a variety of applications, including antibody/antigen binding [20], bacterial cultivation [22], and chemical reaction [23], indicating its significant potential in biosensing applications.

This study reports an OECT-based biosensor that integrates a modified gate electrode within a novel flow-cell device. The channel was fabricated using the screen printing technique with poly(3,4-ethylenedioxythiophene) polystyrene sulfonate (PEDOT:PSS) as the material of choice [24]. The modified gate electrode in the flow-cell device is a gold-coated polyethylene terephthalate (PETE) sterilization filter (0.2- μm pore size). The electrode is inserted into a 3-D printed flow-cell structure, which allows the transport of liquid while accumulating bacteria in test samples.

The flow-cell device exhibited appropriate operational status (gate voltage control) and remained impervious to leakage across a range of flow rates (from 1 to 20 mL/h) and test solutions. To demonstrate the viability of these devices, tests were conducted on three frequently used liquid products (Air Febreze, Tide, and Old SPICE Bodywash), three types of bacteria, and 1- μm silicon oxide microparticles. Sterile solutions of each liquid product were used as controls.

A. Working Principle of Modified Gate OECT Operation

A typical OECT (Fig. 1) consists of the usual three electrodes (gate, source, and drain) and two chemically functional regions—the organic (semi)conductor channel and the electrolyte. For our flow-cell device, Au is used as the contact

material for all three electrodes and PEDOT:PSS is used as the channel material, as it is known for good hole conductivity and electrochemical stability [25].

OECTs conventionally operate in depletion mode (“normally on”) [25], with the source electrode grounded, and the gate and drain electrodes supplied with positive and negative biases, respectively. The drain-to-source channel current (I_{DS}) is modulated (decreased) by the gate voltage (V_{GS}) by causing ions from the electrolyte to penetrate the bulk of the organic channel layer [26], effectively “de-doping” the channel volume. The gate-to-channel equivalent circuit [27] consists of the electrolyte resistance (R_E), and two capacitors are connected in series: the gate–electrolyte capacitance (C_G) and the electrolyte–channel capacitance (C_{CH}). Electrical double layers (EDLs) are formed at the gate–electrolyte and electrolyte–channel interfaces [22], [28].

The presence of the EDL results in a solution (electrolyte) voltage (V_{sol}) applied on the channel that is less than the externally applied gate voltage [13], [19]. The decrease is determined by the ratio of the capacitors across the two EDLs: $\gamma = C_{CH}/C_G$. During the OECT operation, changes occurring on the gate and/or channel result in a solution voltage change ΔV_{sol} , leading to a shift in the output current I_{DS} . When studying this effect, many articles use the term effective gate voltage V_{eff} [21] to represent the gate voltage that would normally be required to yield the same I_{DS} (Fig. 1). In the case of cell presence in the electrolyte, attachment to the OECT drain–source channel (“channel sensing”) will generally result in an increase in I_{DS} and hence in a $V_{eff} < V_{GS}$, as reported by Wei et al. [22]. On the other hand, cell adhesion or presence on the gate electrode results in a decrease in I_{DS} and hence in $V_{eff} > V_{GS}$, as reported by Demuru et al. [15]. This theory can be proven in bacteria testing results in Section III.

II. DESIGN, FABRICATION, AND PROCESSES

A. Channel Design and Fabrication

Ultrawide glass slide (Fisherbrand¹ Extra-Thick Microscope Slides 75 × 50 mm) was selected as the substrate for fabricating the OECT channel, which offers excellent electrical insulation, dimensional stability, surface uniformity, and chemical resistance. Au was used as the electrode contact material and PEDOT:PSS serves as the conducting polymer. A dual-channel OECT has been developed for multifunctional optimization. This advancement increases the yield of device fabrication and endows the device with two distinct capabilities. In preliminary trials, the dual-channel OECT can function as an independent sensor, with one of the channels serving as a gate electrode. In addition, in subsequent experiments, the device can be integrated into a 3-D flow-cell device.

A two-layer covered mask material deposition technique was developed for channel patterning [Fig. 2(a)]. Initially, extra tack frisket adhesive film (Grafix Corp.) is attached to the pre-cleaned glass slide, and then, the electrode block pattern is cut using a laser cutting system (Universal Laser Systems VLS3.50) and removed from the glass slide. Subsequently, the channel block mask is superimposed onto the initial

¹Trademarked.

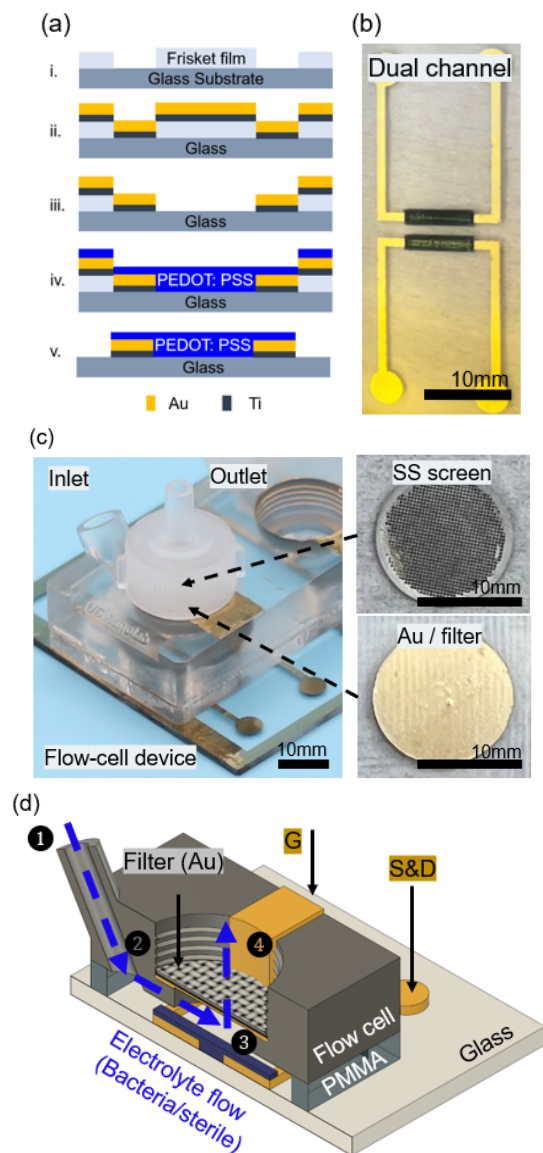


Fig. 2. OECT flow-cell sensor. (a) Dual-channel fabrication process. (b) Photograph of fabricated device. (c) 3-D-printed flow cell incorporating the Au-coated 0.2- μm filter as gate electrode and stainless-steel filter supporting screen. (d) Schematic of flow-cell sensor indicating flow through the device.

pattern (step i). The contact electrode is formed by depositing titanium (20 nm) and Au (60 nm) onto a patterned glass slide using e-beam physical vapor deposition (step ii). The patterned frisket film for the channel is then removed from the sample, establishing the channel gap between source and drain electrodes (step iii). PEDOT:PSS (5.0 wt.%) conductive ink (Millipore Sigma) is printed through a patterned screen printing mask over the channel and electrodes (step iv). Finally, the film mask for the electrode pattern of the device is removed (step v). The channel was postprocessed with 30-min exposure to dimethyl sulfoxide (DMSO) and 10-min curing at 105 °C. The channel dimensions are 0.2 mm in length, 1 mm in width, and 5 μm in thickness. [Fig. 2(b)]. The average resistance across the channel over multiple devices is 75 Ω ($n = 36$ and $\sigma = \pm 5 \Omega$).

B. Flow-Cell Design and Fabrication

The flow-cell sensor is comprised of several key components: dual-channel OECTs on the glass slide substrate, a PMMA intermediate layer, and the flow-cell structure containing the gate electrode and filter. The utilization of a PMMA layer with a thickness of 2 mm serves to protect the channel from damage during assembly of the flow-cell structure while also ensuring that the gate electrode remains consistently positioned above the channel. In addition, this layer acts as a safeguard against any potential leakage within the media flow environment. The flow-cell structure is based on a 3-D model that has been designed and printed using high-temperature resin on a Form 3B SLA 3-D printer (45–60- μm resolution, Formlabs). The design of the flow-cell structure is intended to facilitate the accommodation of Luer-lock tubing connections and the bolt configuration of Sterlitech commercial filter holder caps [Fig. 2(c)]. For the formation of the gate electrode, a 60-nm Au gold layer is deposited onto the hydrophilic polyester (PETE) membrane filter (Sterlitech) with a 0.2- μm pore size and 13 mm diameter. In the process of constructing the flow-cell devices, the laser-cut PMMA pattern is attached to the channel glass plates using a durable adhesive composed of acrylic and glass (10-h curing). The 3-D printed flow-cell structure is applied on top of the PMMA layer using a waterproof superglue (8-h curing). Finally, the device is equipped with the modified filter/gate electrode and an accompanying support screen (13 mm, stainless-steel screen from Sterlitech) in order to secure the modified filter in place during the flow of media.

The operation of the flow-cell device is illustrated in Fig. 2(d).

- 1) Media is introduced into the inlet present on side of the device structure.
- 2) Media flow fills out the testing region, with total volume of 475 μL .
- 3) The modified gate electrode accumulates bacteria on the gate electrode.
- 4) The solution that has undergone filtration is removed through the outlet port.

In the initial device characterization, 10 mL of sterile or bacterial solution was injected into the device at a rate of 20 mL/h, with no leakage occurring. Upon transferring the filtrate onto a nutrient-dense agar medium for cultivation, no discernible bacterial colonies were observed. This test indicates the efficient functionality of the flow-cell device in accumulating bacteria on the gate/filter as well as filtrating all microorganisms from the test solution.

C. Sample Preparation and Testing Procedure

The composition of sterile testing and culture media comprises a combination of commercial household liquid products (10 wt.%) and Dey–Engley (D/E) neutralizing broth (90 wt.%). The household products studied were Air Febreze, Tide, and Old SPICE Bodywash. The incorporation of D/E bouillon into the medium dilutes the preservatives in the liquid products and facilitates consistent bacterial growth in the medium, facilitating a convenient reference for testing concentration.

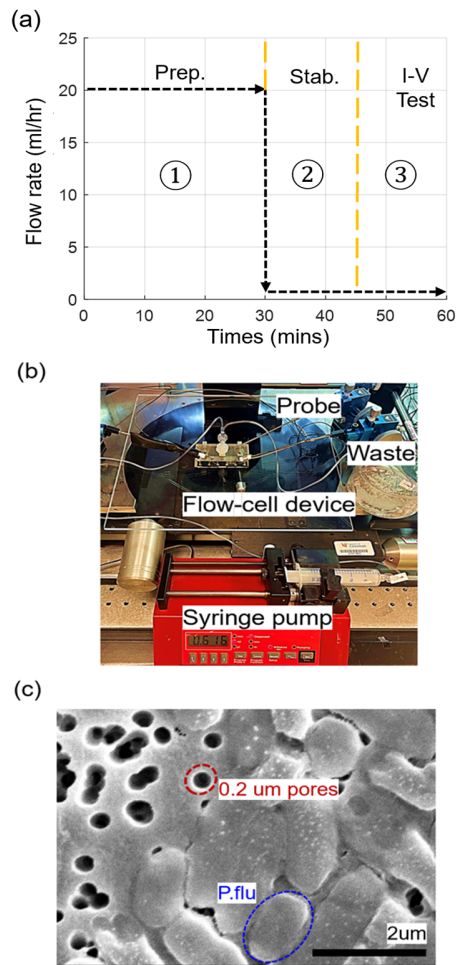


Fig. 3. OECT flow-cell operation. (a) Corresponding flow-rate control during the testing procedure. (b) Testing setup. (c) SEM photograph of a used OECT gate/filter showing $\sim 0.2\text{-}\mu\text{m}$ pores and the presence of a *P. flu* bacterium.

The bacteria used for the tests are *Pseudomonas fluorescens* (*P. flu*), *Escherichia coli* (*E. coli*), and *Staphylococcus aureus* (*S. au*). All three bacterial strains are easily cultivable and have been implicated in food and liquid contamination, as well as being responsible for the majority of bacterial infections in humans [29]. All three bacteria share roughly comparable dimensions ($\sim 0.5\text{--}1\ \mu\text{m}$ width and $\sim 1.5\text{--}2.5\ \mu\text{m}$ length) [30] and can be filtered using a $0.2\text{-}\mu\text{m}$ filter.

Before testing, the sample media is brought to room temperature for 30 min. Serial dilution is used to control the bacteria concentration. To our best efforts, serial dilution can control the bacteria concentration within approximately an order of magnitude, hence the slight variation between the concentrations of various bacteria. OECT flow-cell testing operation consists of three steps [Fig. 3(a)].

- 1) *Preparation*: Using a programmed New Era syringe pump, 10 mL of testing sterile or bacteria solution is introduced into the flow cell system at a rate of 20 mL/h.
- 2) *Stabilization*: Reducing the flow rate to 1 mL/h over a period of 15 min to reach a stable pressure within the flow cell.

- 3) *Testing*: Maintaining a flow rate of 1 mL/h to keep microorganisms confined on the gate/filter, while standard current–voltage ($I\text{--}V$) curve traces are performed on the OECT. For example, when testing a 5×10^3 CFU/mL bacteria solution, approximately 50 000 CFU of bacteria are accumulated on the gate/filter by the end of the flow-cell testing operation. Fig. 3(b) shows a photograph of the flow-cell test setup in an electrical test probe system.

Fig. 3(c) shows an SEM microphotograph of a decommissioned filter after use in the flow-cell system showing the $0.2\text{-}\mu\text{m}$ filter pores and the presence of a *P. flu* bacterium.

III. RESULTS AND DISCUSSION

A. Planar Channel Sensing

As discussed in Section II, the dual-channel OECT design provides a useful benefit of having two side-by-side devices that can provide the function of a bacteria sensor. One of the channels is utilized as the gate electrode of the device for current modulation, while the other serves as the sensing channel, as seen in Fig. 2(b). The initial testing outcomes were obtained utilizing a planar OECT in conjunction with a laser-cut acrylic well (8 mm in diameter and 5 mm in height) to contain the test solutions over the OECT.

The testing procedure is carried out using the $I\text{--}V$ curve-trace characterization method. V_{GS} applied on the gate electrode is increased in 0.1 V steps from 0 to 1 V. At every fixed V_{GS} , the channel current (I_{DS}) is measured for applied drain-to-source voltage (V_{DS}) changing from 0 to -0.5 V at -0.05-V steps. As a result of applying a negative V_{DS} bias across the channel, the entire I_{DS} response is in negative value. For convenience of observation and parallel comparison with subsequent results, we used the absolute value of the output current $|I_{DS}|$ for displaying the resulting data plots. Fig. 4(a) shows good transistor behavior of the planar OECT, where increasing the channel potential results in increasing $|I_{DS}|$, while increasing the gate potential results in decreasing $|I_{DS}|$ (switching OFF the transistor) [28]. The relationship between the OECT output current $|I_{DS}|$ and the modulating gate voltage V_{GS} in the presence of various bacteria concentrations is shown in the $I\text{--}V$ curve plot of Fig. 4(b) for a fixed V_{DS} of -0.3 V. (In $I\text{--}V$ curve tracing, it was observed that V_{GS} produces good distinguishable switching behavior at $V_{DS} = -0.3$ V.)

For planar OECT testing, $450\ \mu\text{L}$ of sample solution is pipetted into the acrylic well on top of the OECT dual SD channel. The $I\text{--}V$ characterization test is performed 45 min after the sample solution is inserted. OECT $I\text{--}V$ characteristics for sterile D/E broth solution and for different concentrations of *P. flu* solutions in D/E broth are shown in Fig. 4(b). The transfer characteristics (I_{DS} versus V_{GS}) in Fig. 4(b) show the normal OECT “switching OFF” behavior where the amplitude of I_{DS} decreases with increasing V_{GS} values across all instances. At each applied V_{GS} voltage step, the plot shows that solutions with high bacteria concentrations (10^7 and 10^9 CFU/mL) have higher $|I_{DS}|$ current, which separate from sterile solution. In the planar OECT “channel sensing” mode used here, sources that can cause the shift of I_{DS} are solution cations that redox the channel [19] and biofilm formation at

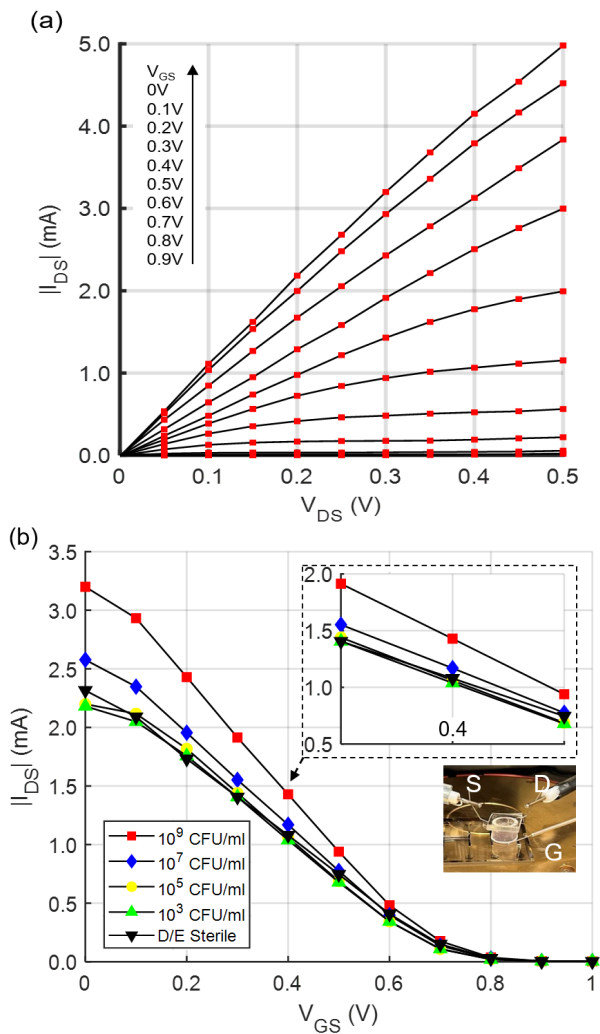


Fig. 4. OECT planar channel bacteria sensing. (a) I - V characteristic (I_{DS} versus V_{DS}) of OECT with 10^9 CFU/mL of bacteria at different applied V_{GS} . (b) Transistor transfer characteristics (I_{DS} versus V_{GS}) for sterile and different concentration ranges of *P. flu* solutions, the inset shows I_{DS} at $V_{GS} = 0.3$ – 0.5 V.

the channel [13]. As discussed previously in Section I, bacteria adhesion at the channel results in a V_{eff} offset, which leads to I_{DS} amplitude decrease [22].

The main contributing factor to this $|I_{DS}|$ increment at higher bacteria concentration is the depressed redox reaction of the organic channel. Bacteria tend to aggregate at the OECT surface due to their charged state [31] and their slightly higher density versus the electrolyte solution [32]. As higher bacteria concentrations are introduced, a greater fraction of the channel surface will be occupied by bacteria preventing solution cations from reaching the PEDOT:PSS channel. In addition, the negative charges on the surface of bacteria can change the ionic strength in the EDL [12], reducing the number of cations penetrating the underlying organic layer [22]. Therefore, with increased bacteria concentration, the effective impact of applied V_{GS} on the channel is reduced; in other words, a higher gate voltage is required to obtain the original channel current (i.e., the “no bacteria” case). Conversely, for a fixed applied

V_{GS} , bacteria on the channel result in an increase in $|I_{DS}|$ output. In the channel sensing case, since there is no external pressure to drive the bacteria toward the channel nor a specific bonding agent to capture them, it is likely that the bacteria fraction present on the channel is significantly less than the total amount of bacteria available, thereby resulting in reduced sensitivity. In addition to adhesion to the channel, bacteria can also attach to the gate area. In our dual-channel planar design, the size of the OECT gate area is the same as the channel area, resulting in bacteria on the channel being the dominant component and, hence, producing an increasing trend in I_{DS} with bacteria concentration. This is further discussed in more detail in Section III-B. In summary, while the dual-channel planar OECT approach has good capability to detect bacteria at elevated concentrations, it has limited usefulness for low-level bacteria sensing.

B. Gate Sensing Using the Flow-Cell Device

To improve the detection of low levels of bacteria in fluid products, we have investigated a flow-cell device in which bacteria can be actively accumulated on the gate electrode of the OECT during fluid flow through the device.

We have tested three major bacteria strains (*P. flu*, *E. coli*, and *S. au*) in three common liquid household products (Air Febreze, Tide, and Old SPICE Bodywash) using the flow-cell device approach. Each combination of bacteria type and liquid product is performed in triplicate ($n = 3$).

A total of 36 flow-cell devices were subjected to testing and characterization under 12 distinct solution conditions (including sterile product solutions). In addition, we investigated the use of $1\text{-}\mu\text{m}$ silica particles (Sigma Aldrich) to mimic the size of the bacteria but without the functionality of the bacterium membrane. Equal volume concentration of SiO_2 micro-beads as that of bacteria is applied to the flow-cell operation.

The OECT transistor transfer characteristics (I_{DS} versus V_{GS}) under these various solution combinations are shown in Fig. 5 for a fixed $V_{DS} = -0.3$ V. The bacteria concentration in all cases is within a similar range of $(\sim 5\text{--}10) \times 10^3$ CFU/mL. As shown in Fig. 5, the amplitude of I_{DS} for both bacteria and sterile solutions is comparable at $V_{GS} = 0$ V and decreases to effectively zero (reduction by three orders of magnitude) at $V_{GS} = 1$ V. This current shift demonstrates that flow-cell devices in depletion mode have excellent channel-gate voltage modulation. The difference in starting I_{DS} amplitude ($V_{GS} = 0$ V) between testing media is due to the conductivity of the electrolyte. Based on our conductivity measurements ($n = 5$) using 10% solutions at 20°C , Bodywash in D/E broth has the highest conductivity (11.2 mS/cm), followed by Tide (8.4 mS/cm) and Febreze (7.2 mS/cm). Introducing 10^3 -CFU/mL bacteria resulted in no noticeable change in conductivity for all three media. Solutions with a higher conductivity contain higher ion concentration, which leads to a more effective OECT channel de-doping process. Thus, a higher conductivity solution results in a lower OECT output current, as both our results (Fig. 5) and other reports demonstrated [12], [21].

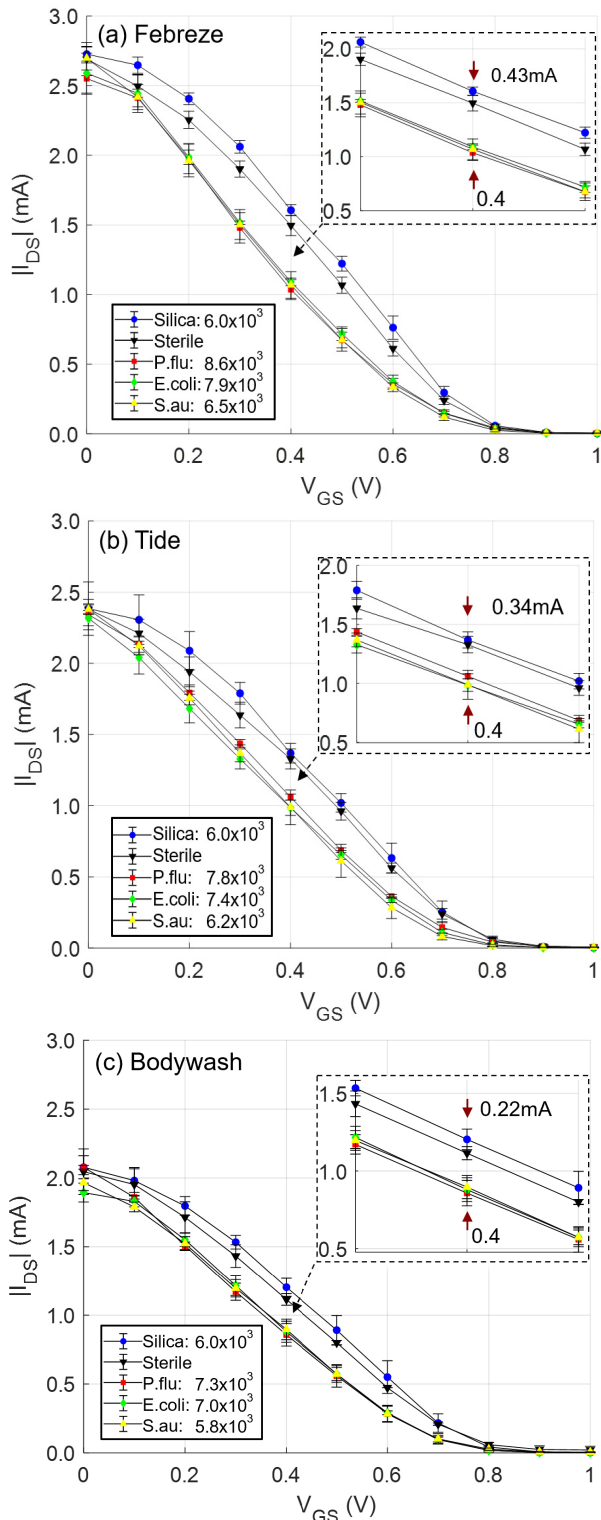


Fig. 5. Gate sensing in OECT flow-cell devices—transistor transfer characteristics (I_{DS} versus V_{GS}) in the absence (sterile solutions) and presence of three individual bacteria types (*P. flu.*, *E. coli*, and *S. au.*) in three household liquid product media (10% in buffer solution). (a) Febreze. (b) Tide. (c) Bodywash. $V_{DS} = -0.3$ V, $n = 3$. The inset shows I_{DS} at $V_{GS} = 0.3$ – 0.5 V. The range bar represents the standard deviation for repeated measurements under the same conditions, same as in the following plots.

In general, a clear differentiation in I_{DS} separation is evident between the sterile and bacteria-containing solutions for all three product-type media. For the solution containing silica

TABLE I
LOD COMPARISON FOR OECT BACTERIA/CELL DETECTION

Detection Mechanism	LOD (CFU/ml)	Types of bacteria/cell
Antibody-binding on PEDOT: PSS channel ^[12]	10^3	<i>Escherichia coli</i>
Antibody capture on Au ink-coated gate ^[15]	10^5	<i>Escherichia coli</i>
pH changes based on cell growth ^[17]	10^5	<i>Micrococcus Luteus</i>
Anticancer drug response ^[14]	10^5	<i>Adenocarcinoma cell line</i>
Light and salt treatment ^[22]	10^5	<i>Haematococcus pluvialis</i>
Accumulation on gate	10^3	<i>E.coli</i> , <i>P.flu</i> and <i>S.au</i>

nanoparticles, the overall I_{DS} versus V_{GS} shows a similar trend to the sterile solution case, but with a slightly larger current. This is likely due to accumulation of the dielectric particles on the gate electrode reducing the gate modulating effect on the channel current [33]. In contrast, all three types of bacterial solutions produce a faster decreasing trend. As an example, at $V_{GS} = 0.4$ V, a difference in current flow of 0.43, 0.34, and 0.22 mA is measured between sterile solution and 10^3 -CFU/mL bacteria solutions containing in Febreze, Tide, and Bodywash, respectively. This difference of $\sim 25\%$ in current clearly indicates that the gate sensing flow cell is capable of detecting bacteria in the concentration range of 10^3 CFU/mL and probably smaller.

Table I summarizes recently published articles related to OECT on bacteria/cell detection. To the best of our knowledge, we have not found any literature that can achieve lower than 10^3 -CFU/mL limit of detection (LOD) in broad bacteria sensing. Compared with typical bacteria-contaminated media (10^9 CFU/mL), 10^3 CFU/mL is a promising broad bacteria detection capability.

As discussed in Section I, the adhesion of bacteria on the gate results in a higher capacitance due to increasing charge on the surface of the electrode [20]. In this case, the gate electrode exhibits a stronger modulating effect on the PEDOT:PSS channel. At a given value of V_{GS} , the bacteria test solution has higher V_{sol} (and V_{eff}) applied on the channel, thus reducing the output I_{DS} current. Thus, in contrast to channel sensing using the planar OECT, the gate sensing approach using the flow cell results in the opposite trend in terms of I_{DS} versus bacteria concentration, with the bacteria solutions resulting in a lower I_{DS} compared to sterile solutions. Further examination of the gate sensing method is discussed in Section III-C.

C. Transconductance Peak Shift Due to Bacteria Adhesion

In order to provide additional clarification regarding the sensing mechanisms in the flow-cell device, a transconductance plot was generated utilizing bacterial data obtained from Fig. 5 and the standard transconductance equation [34]: $g_m = \partial I_{DS} / \partial V_{GS}$, g_m is a critical performance parameter in all gate-controlled transistors, including MOSFETs, OFETs, and OECTs. g_m represents the transistor's amplification factor as

well as the system's sensitivity when comparing performance of various OECTs [34]. For OECTs, g_m has a bell-shaped dependence on the applied V_{GS} , from active channel de-doping process (low V_{GS} , g_m increasing) to I_{DS} saturation (high V_{GS} , g_m decreasing) [19], [28], as evidenced also by our devices (Fig. 6). The point of maximum g_m curve can serve as a means to identify the device's optimal external operating parameters (V_{DS} and V_{GS}) [35]. For sterile samples of the three types of media, the g_m peak occurs at V_{GS} values of ~ 0.5 – 0.55 V. For the case of the silica particle solutions, the g_m peak occurs at slightly larger values of $V_{GS} \sim 0.65$ V. By contrast, for the bacteria-containing solutions, a significant shift in the g_m peak is observed in the opposite direction, occurring at a lower V_{GS} of ~ 0.2 – 0.3 V. This 0.3-V shift is caused by the attachment of bacteria to the Au-coated gate electrode.

In flow-cell bacteria sensing, operating in the low V_{GS} region (0.1–0.3 V) optimizes the performance as the bacteria will produce a stronger gating on the transistor I_{DS} output. To investigate this g_m peak shifting effect, we replaced the Au-coated filter membrane with an Ag/AgCl gate electrode and performed the same flow-cell sensing operation. The output results and characteristics of flow-cell operation for different gate materials are shown in Fig. 7. In Fig. 7(a), one can observe that for sterile solutions, the use of the Ag/AgCl electrode significantly reduces the output current compared to the Au gate electrode operation. This is similar to, but more pronounced, the effect of bacteria on the gate resulting in an I_{DS} decrease. For operation with the Ag/AgCl electrode, the g_m peak is found at a significantly lower value of V_{GS} than for Au electrode operation and closer to bacteria-on-Au electrode gate operation [Fig. 7(b)]. Bacteria accumulation on the gate is similar to switching the material of OECT gate electrode from a polarizable electrode (Au) to a nonpolarizable electrode (Ag/AgCl reference electrode) [36].

To explain this result, the difference between the OECT transconductance for modified gate electrode (bacteria-on-Au and Ag/AgCl electrode) and the conventional Au gate is shown in Fig. 7(c) as a function of gate voltage. The plot indicates that at very high voltages, $g_{m,diff}$ is nearly zero, which is expected since the OECT in the saturated “OFF” cases (independent of gate voltage). At low but increasing applied voltage, values of $g_{m,diff}$ are positive indicating that “nonpolarizable” gate electrode is preferred and producing efficient gating. A clear shift is observed from positive to negative, indicating that the device is now operating in the “polarizable” gate electrode region. In this region, a higher gate voltage is required to address the higher potential gap between the gate to the channel. Fig. 7(c) provides an interesting approach for determining the effect of other electrode materials on the OECT transconductance characteristics [19].

From the EDL ion circuit standpoint, V_{sol} will shift to a higher value [37] when bacteria attach on the gate electrode due to its surface charges [38] and related conformational changes [20], the overall change in V_{sol} can be summarized as an external offset voltage. The additional offset voltage increases the overall V_{eff} [21]; with higher V_{eff} , redox reaction on the organic layer will have a higher gain and more cations

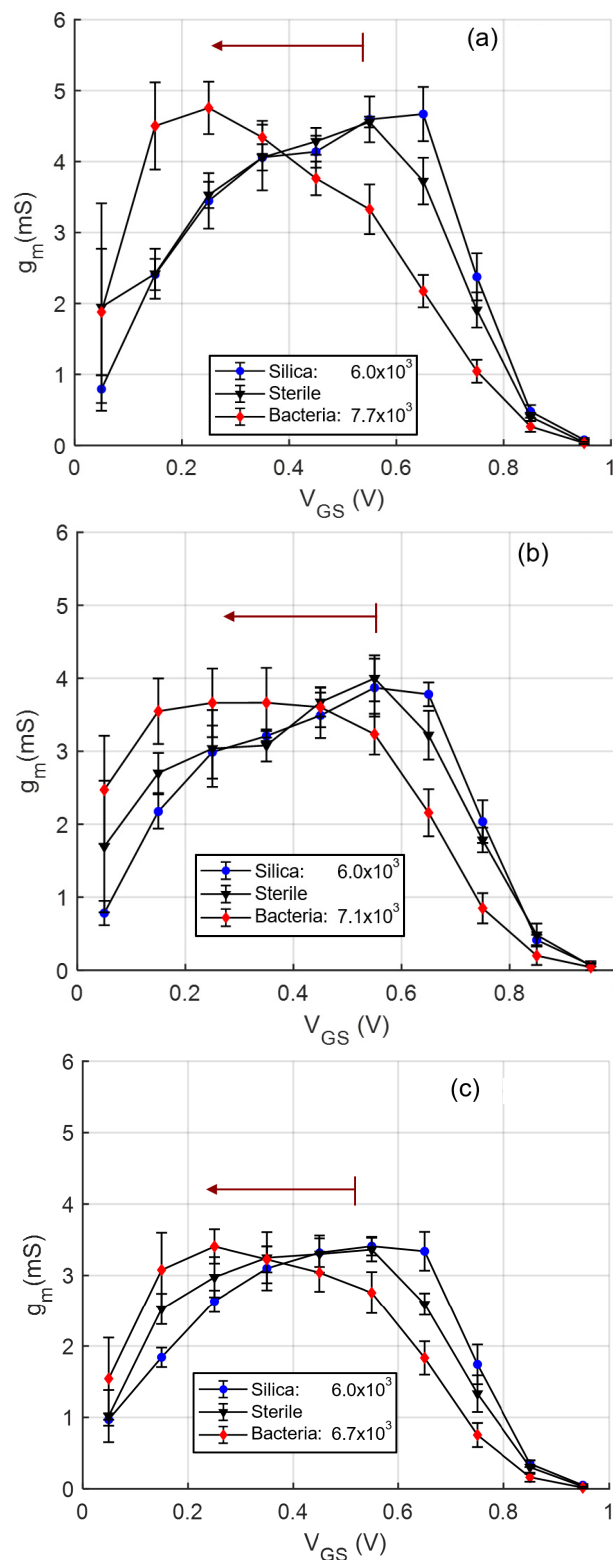


Fig. 6. Transconductance characteristics of gate sensing OECTs for sterile, silica NPs, and average of all three types of bacteria in liquid product media. (a) Febreze. (b) Tide. (c) Bodywash. $V_{DS} = -0.3$ V and $n = 3$.

will penetrate the bulk of the organic layer (smaller $|I_{DS}|$). In other words, bacteria on gate result in a higher V_{GS} efficiency in channel current modulation, and less applied V_{GS} is required to obtain the OECT's optimized performance (at

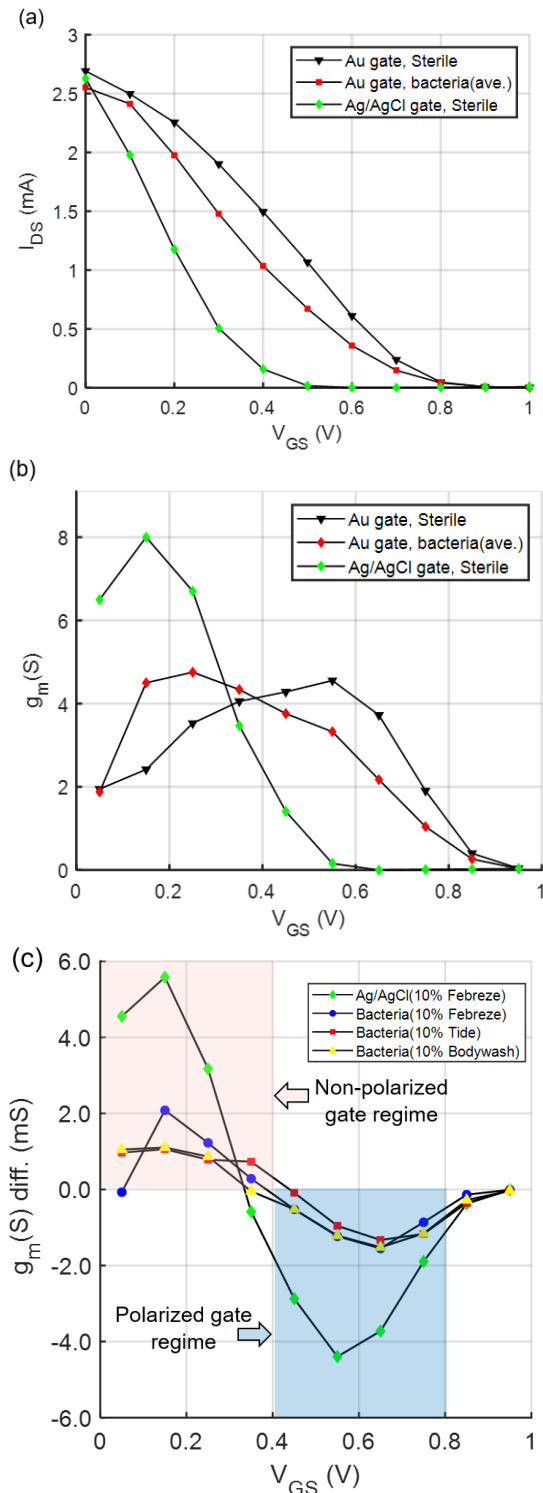


Fig. 7. Effect of gate electrode material and type on OECT gate sensing operation for Au electrode with and without bacteria present, and for Ag/AgCl reference electrode. (a) Transfer characteristics (I_{DS} versus V_{GS}) of sterile solution (10% Febreze in D/E) with Au gate, bacteria (103 CFU/mL, average of three types) with Au gate and sterile solution with Ag/AgCl gate electrode. (b) Corresponding transconductance. (c) Transconductance difference between Au electrode operation with bacteria present (average for all three bacterium types, 103 CFU/mL) versus sterile solutions of 10% Febreze, 10% Tide, and 10% Bodywash; also difference between Ag/AgCl and Au gate electrodes for sterile 10% Febreze only. $V_{DS} = -0.3$ V.

$g_{m,peak}$). This also explains the trend in Fig. 7(c), and g_m shifts to positive value at lower gate operating voltage due to

bacteria attachment on Au gate. g_m peak shift will necessitate additional investigation in future works on the subject.

IV. CONCLUSION

In summary, we have reported a novel flow-cell sensor for broad detection of bacteria based on a gate sensing 3-D OECT approach. The device has been demonstrated to be capable of detecting several types of bacteria (*P. flu*, *E. coli*, and *S. au*) potentially present in household liquid product mixtures. The test results show that using the flow-cell approach accumulating bacteria on the gate electrode (“gate sensing”) will result in an I_{DS} amplitude change (decrease) that can be used to readily distinguish between sterile and bacterial solutions. To demonstrate the working mechanism of the flow-cell method, the corresponding transconductance curve is analyzed, revealing that bacteria adhesion on the gate electrode causes a g_m peak shift to lower V_{GS} , due to the slope change in I_{DS} . The flow-cell filtration and OECT gate sensing approach has the capability to identify a diverse range of bacteria, encompassing both gram-positive and gram-negative strains, across multiple testing media.

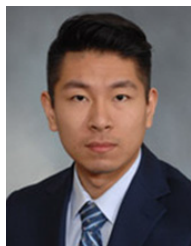
ACKNOWLEDGMENT

The authors appreciate William Gore, Terry Amoroso, and Neil Lewis for many helpful technical discussions. They also thank Spencer Kohorst for developing the initial bacteria culturing protocol.

REFERENCES

- [1] H. D. Kusumaningrum, M. M. Van Putten, F. M. Rombouts, and R. R. Beumer, “Effects of antibacterial dishwashing liquid on foodborne pathogens and competitive microorganisms in kitchen sponges,” *J. Food Protection*, vol. 65, no. 1, pp. 61–65, Jan. 2002.
- [2] L. Váradi et al., “Methods for the detection and identification of pathogenic bacteria: Past, present, and future,” *Chem. Soc. Rev.*, vol. 46, no. 16, pp. 4818–4832, 2017.
- [3] N. C. Cady, S. Stelick, M. V. Kunnakkam, Y. Liu, and C. A. Batt, “A microchip-based DNA purification and real-time PCR biosensor for bacterial detection,” in *Proc. SENSORS*, Oct. 2004, pp. 1191–1194.
- [4] K. J. AbuHassan et al., “Automatic diagnosis of tuberculosis disease based on Plasmonic ELISA and color-based image classification,” in *Proc. 39th Annu. Int. Conf. IEEE Eng. Med. Biol. Soc.*, Jul. 2017, pp. 4512–4515.
- [5] J. Rivnay, S. Inal, A. Salleo, R. M. Owens, M. Berggren, and G. G. Malliaras, “Organic electrochemical transistors,” *Nature Rev. Mater.*, vol. 3, no. 2, pp. 1–14, 2018.
- [6] E. Zeglio and O. Inganäs, “Active materials for organic electrochemical transistors,” *Adv. Mater.*, vol. 30, no. 44, Nov. 2018, Art. no. 1800941.
- [7] A. Moudgil and W. L. Leong, “Highly sensitive transistor sensor for biochemical sensing and health monitoring applications: A review,” *IEEE Sensors J.*, vol. 23, no. 8, pp. 8028–8041, Apr. 2023.
- [8] M. Sessolo, J. Rivnay, E. Bandiello, G. G. Malliaras, and H. J. Bolink, “Ion-selective organic electrochemical transistors,” *Adv. Mater.*, vol. 26, no. 28, pp. 4803–4807, 2014.
- [9] S. T. Keene, D. Fogarty, R. Cooke, C. D. Casadevall, A. Salleo, and O. Parlak, “Wearable organic electrochemical transistor patch for multiplexed sensing of calcium and ammonium ions from human perspiration,” *Adv. Healthcare Mater.*, vol. 8, no. 24, Dec. 2019, Art. no. 1901321.
- [10] Y. Kim et al., “A glucose sensor based on an organic electrochemical transistor structure using a vapor polymerized poly(3,4-ethylenedioxythiophene) layer,” *Jpn. J. Appl. Phys.*, vol. 49, no. 1, Jan. 2010, Art. no. 01AE10.
- [11] X. Ma et al., “OFET and OECT, two types of organic thin-film transistor used in glucose and DNA biosensors: A review,” *IEEE Sensors J.*, vol. 22, no. 12, pp. 11405–11414, Jun. 2022.

- [12] R.-X. He et al., "Detection of bacteria with organic electrochemical transistors," *J. Mater. Chem.*, vol. 22, no. 41, pp. 22072–22076, 2012.
- [13] E. Frantz, J. Huang, D. Han, and A. J. Steckl, "The effect of nutrient broth media on PEDOT:PSS gated OECTs for whole-cell bacteria detection," *Biosensors Bioelectron.*, X, vol. 12, Dec. 2022, Art. no. 100268.
- [14] A. Romeo et al., "Drug-induced cellular death dynamics monitored by a highly sensitive organic electrochemical system," *Biosensors Bioelectron.*, vol. 68, pp. 791–797, Jun. 2015.
- [15] S. Demuru, A. Marett, W. Kooli, P. Junier, and D. Briand, "Flexible organic electrochemical transistor with functionalized inkjet-printed gold gate for bacteria sensing," in *Proc. 20th Int. Conf. Solid-State Sensors, Actuators, Microsystems Eurosensors*, Jun. 2019, pp. 2519–2522.
- [16] D. A. Bernards and G. G. Malliaras, "Steady-state and transient behavior of organic electrochemical transistors," *Adv. Funct. Mater.*, vol. 17, no. 17, pp. 3538–3544, Nov. 2007.
- [17] K. Matsuura, Y. Asano, A. Yamada, and K. Naruse, "Detection of micrococcus luteus biofilm formation in microfluidic environments by pH measurement using an ion-sensitive field-effect transistor," *Sensors*, vol. 13, no. 2, pp. 2484–2493, Feb. 2013.
- [18] S.-M. Kim et al., "Influence of PEDOT:PSS crystallinity and composition on electrochemical transistor performance and long-term stability," *Nature Commun.*, vol. 9, no. 1, p. 3858, Sep. 2018.
- [19] P. Lin, F. Yan, and H. L. W. Chan, "Ion-sensitive properties of organic electrochemical transistors," *ACS Appl. Mater. Interfaces*, vol. 2, no. 6, pp. 1637–1641, Jun. 2010.
- [20] S. Demuru et al., "Antibody-coated wearable organic electrochemical transistors for cortisol detection in human sweat," *ACS Sensors*, vol. 7, no. 9, pp. 2721–2731, Sep. 2022.
- [21] D. A. Bernards, D. J. Macaya, M. Nikolou, J. A. DeFranco, S. Takamatsu, and G. G. Malliaras, "Enzymatic sensing with organic electrochemical transistors," *J. Mater. Chem.*, vol. 18, no. 1, pp. 116–120, 2008.
- [22] W. Wei et al., "A novel organic electrochemical transistor-based platform for monitoring the senescent green vegetative phase of haematococcus pluvialis cells," *Sensors*, vol. 17, no. 9, p. 1997, Aug. 2017.
- [23] N. Y. Shim et al., "All-plastic electrochemical transistor for glucose sensing using a ferrocene mediator," *Sensors*, vol. 9, no. 12, pp. 9896–9902, Dec. 2009.
- [24] G. B. Tseghai et al., "PEDOT:PSS-based conductive textiles and their applications," *Sensors*, vol. 20, no. 7, p. 1881, 2020.
- [25] F. Alhashmi et al., "Review on PEDOT:PSS-based conductive fabric," *ACS Omega*, vol. 7, no. 40, pp. 35371–35386, 2022.
- [26] M. Moser, J. F. Ponder, A. Wadsworth, A. Giovannitti, and I. McCulloch, "Materials in organic electrochemical transistors for bioelectronic applications: Past, present, and future," *Adv. Funct. Mater.*, vol. 29, no. 21, May 2019, Art. no. 1807033.
- [27] A. J. Bard, L. R. Faulkner, and H. S. White, *Electrochemical Methods: Fundamentals and Applications*. New York, NY, USA: Wiley, 1980.
- [28] P. Lin, F. Yan, J. Yu, H. L. W. Chan, and M. Yang, "The application of organic electrochemical transistors in cell-based biosensors," *Adv. Mater.*, vol. 22, no. 33, pp. 3655–3660, Sep. 2010.
- [29] S. C. Davies, T. Fowler, J. Watson, D. M. Livermore, and D. Walker, "Annual report of the chief medical officer: Infection and the rise of antimicrobial resistance," *Lancet*, vol. 381, no. 9878, pp. 1606–1609, May 2013.
- [30] S. S. Board and N. R. Council, *Size Limits of Very Small Microorganisms: Proceedings of a Workshop*. Washington, DC, USA: National Academies Press, 1999.
- [31] H. N. Kim, Y. Hong, I. Lee, S. A. Bradford, and S. L. Walker, "Surface characteristics and adhesion behavior of *Escherichia coli* O157:H7: Role of extracellular macromolecules," *Biomacromolecules*, vol. 10, no. 9, pp. 2556–2564, Sep. 2009.
- [32] M. Loferer-Krossbacher, J. Klima, and R. Psenner, "Determination of bacterial cell dry mass by transmission electron microscopy and densitometric image analysis," *Appl. Environ. Microbiol.*, vol. 64, no. 2, pp. 688–694, Feb. 1998.
- [33] F. Ciccoira, M. Sessolo, O. Yaghmazadeh, J. A. DeFranco, S. Y. Yang, and G. G. Malliaras, "Influence of device geometry on sensor characteristics of planar organic electrochemical transistors," *Adv. Mater.*, vol. 22, no. 9, pp. 1012–1016, Mar. 2010.
- [34] D. Ohayon, V. Druet, and S. Inal, "A guide for the characterization of organic electrochemical transistors and channel materials," *Chem. Soc. Rev.*, vol. 52, no. 3, pp. 1001–1023, 2023.
- [35] P. R. Paudel, J. Tropp, V. Kaphle, J. D. Azoulay, and B. Lüssem, "Organic electrochemical transistors—From device models to a targeted design of materials," *J. Mater. Chem. C*, vol. 9, no. 31, pp. 9761–9790, 2021.
- [36] M. Sophocleous and J. K. Atkinson, "A review of screen-printed silver/silver chloride (Ag/AgCl) reference electrodes potentially suitable for environmental potentiometric sensors," *Sens. Actuators A, Phys.*, vol. 267, pp. 106–120, Nov. 2017.
- [37] L. V. Lingstedt et al., "Monitoring of cell layer integrity with a current-driven organic electrochemical transistor," *Adv. Healthcare Mater.*, vol. 8, no. 16, Aug. 2019, Art. no. 1900128.
- [38] J. Li and L. A. McLandsborough, "The effects of the surface charge and hydrophobicity of *Escherichia coli* on its adhesion to beef muscle," *Int. J. Food Microbiol.*, vol. 53, nos. 2–3, pp. 185–193, Dec. 1999.



Jingchu Huang (Member, IEEE) received the bachelor's degree in electrical engineering from the University of Cincinnati, Cincinnati, OH, USA, in 2019, where he is currently pursuing the Ph.D. degree with the Department of Electrical and Computer Engineering.

His main research interests include semiconductor fabrication and organic transistors.



Daewoo Han received the master's degree in telecommunications engineering from Hoseo University, Cheonan, South Korea, in 1998, and the Ph.D. degree from the Department of Electrical and Computer Engineering, University of Cincinnati, Cincinnati, OH, USA, in 2010.

He has conducted research in nanotechnology and point-of-care diagnostics, especially on developing multifunctional nanofiber applications, which led to multiple breakthrough findings and outcomes. He is currently working as a Senior Research Associate and an Adjunct Instructor with the University of Cincinnati. He is heavily involved in a variety of externally funded multidisciplinary projects.



Andrew J. Steckl (Life Fellow, IEEE) received the B.S.E. degree in electrical engineering from Princeton University, Princeton, NJ, USA, in 1968, and the M.Sc. and Ph.D. degrees from the University of Rochester, Rochester, NY, USA, in 1970 and 1973, respectively.

From 1972 to 1976, he worked on infrared devices at Honeywell, Lexington, MA, USA, and charge-coupled devices at Rockwell, Anaheim, CA, USA. In 1976, he joined the Electrical, and Systems Engineering Department, Rensselaer Polytechnic Institute, Troy, NY, USA, where he developed a research program in microfabrication of Si devices. In 1981, he founded the Center for Integrated Electronics, a multidisciplinary academic center focused on VLSI research and teaching. In 1988, he joined the Electrical and Computer Engineering Department, University of Cincinnati, Cincinnati, OH, USA, as an Ohio Eminent Scholar and a Gieringer Professor of Solid-State Microelectronics. Previously, his research focused on optoelectronic devices, including rare-earth doped wide bandgap semiconductors. Current research includes a variety of biosensors for point-of-care/use diagnostics, and electrospinning of complex fiber membranes for chemical and biomedical applications. His research has resulted in over 450 publications and 28 patents.

Dr. Steckl is a Fellow of the American Association for the Advancement of Science and the National Academy of Inventors. He received the Electronics and Photonics Award of the Electrochemical Society for Outstanding Achievements in Optoelectronic Materials and Devices in 2022.